

Journal of Visualized Experiments

A rhodopsin transport assay by high-content imaging analysis

--Manuscript Draft--

| | |
|--|---|
| Article Type: | Invited Methods Article - JoVE Produced Video |
| Manuscript Number: | JoVE58703R2 |
| Full Title: | A rhodopsin transport assay by high-content imaging analysis |
| Keywords: | High-content imaging, misfolded protein, rhodopsin transport, retinitis pigmentosa, pharmacological chaperone, immunostaining |
| Corresponding Author: | Yuanyuan Chen UNITED STATES |
| Corresponding Author's Institution: | |
| Corresponding Author E-Mail: | Yuanyuan.Chen@pitt.edu |
| Order of Authors: | Bing Feng Xujie Liu Yuanyuan Chen |
| Additional Information: | |
| Question | Response |
| Please indicate whether this article will be Standard Access or Open Access. | Standard Access (US\$2,400) |
| Please indicate the city, state/province, and country where this article will be filmed . Please do not use abbreviations. | Pittsburgh, PA |

TITLE:

A Rhodopsin Transport Assay by High-Content Imaging Analysis

AUTHORS AND AFFILIATIONS:

Bing Feng¹, Xujie Liu¹ and Yuanyuan Chen^{1,2}

¹Department of Ophthalmology, University of Pittsburgh, Pittsburgh, PA, USA

²McGowan Institute for Regenerative Medicine, University of Pittsburgh, Pittsburgh, PA, USA

Corresponding Author:

Yuanyuan Chen

cheny1@pitt.edu

Tel: (412)-624-5444

Email Addresses for Co-authors:

Bing Feng (bingfeng@pitt.edu)

Xujie Liu (xujieliu@pitt.edu)

KEYWORDS:

High-content imaging, misfolded protein, rhodopsin, retinitis pigmentosa, pharmacological chaperone, immunostaining

SUMMARY:

Here, we described a high-content imaging method to quantify the transport of rhodopsin mutants associated with retinitis pigmentosa. A multiple-wavelength scoring analysis was used to quantify rhodopsin protein on the cell surface or in the whole cell.

ABSTRACT:

Rhodopsin misfolding mutations lead to rod photoreceptor death that is manifested as autosomal dominant retinitis pigmentosa (RP), a progressive blinding disease that lacks effective treatment. We hypothesize that the cytotoxicity of the misfolded rhodopsin mutant can be alleviated by pharmacologically stabilizing the mutant rhodopsin protein. The P23H mutation, among the other Class II rhodopsin mutations, encodes a structurally unstable rhodopsin mutant protein that is accumulated in the endoplasmic reticulum (ER), whereas the wild type rhodopsin is transported to the plasma membrane in mammalian cells. We previously performed a luminescence-based high-throughput screen (HTS) and identified a group of pharmacological chaperones that rescued the transport of the P23H rhodopsin from ER to the plasma membrane. Here, using an immunostaining method followed by a high-content imaging analysis, we quantified the mutant rhodopsin protein amount in the whole cell and on the plasma membrane. This method is informative and effective to identify true hits from false positives following HTS. Additionally, the high-content image analysis enabled us to quantify multiple parameters from a single experiment to evaluate the pharmacological properties of each compound. Using this assay, we analyzed the effect of 11 different compounds towards six RP associated rhodopsin mutants, obtaining a 2-D pharmacological profile for a quantitative and qualitative understanding about the structural stability of these rhodopsin mutants and efficacy of different compounds

towards these mutants.

INTRODUCTION:

Protein misfolding is involved in muscular dystrophy, neural degenerations, as well as blinding diseases, including retinitis pigmentosa (RP)¹. RP is an inherited and progressive retinal degeneration associated with mutations in over 60 genes affecting the function and homeostasis of rod photoreceptors or the retinal pigmented epitheliums (RPEs)^{2,3}. No effective treatment is currently available for RP. *Rhodopsin* mutations account for about 25-30% of autosomal dominant (ad) RP cases. Among the more than 150 *Rhodopsin* mutations⁴ (Human Gene Mutation Database, <http://www.hgmd.cf.ac.uk/>), the Class II mutations cause the structural instability of the rhodopsin protein that contributes to the rod photoreceptor death and vision loss⁵⁻⁸. The P23H is the most frequent *Rhodopsin* mutation in North America, which is also a typical example of the Class II rhodopsin mutations^{9,10}. Due to its inherent structural instability, the misfolded rhodopsin is accumulated in the endoplasmic reticulum (ER) in mammalian cells, whereas the wild type rhodopsin is located on the plasma membrane⁵. The misfolded rhodopsin P23H mutant exhibits dominant negative cytotoxicity that is not due to haploinsufficiency, but is related to the activation of ER associated protein degradation pathway and the interrupted rod outer segment organization. To alleviate rod photoreceptor cell stress, one strategy is to stabilize the native folding of the mutant rhodopsin using a pharmacological chaperone.

To achieve this goal, we performed a cell-based high-throughput screen (HTSs)¹¹⁻¹³ using a β -galactosidase fragment complementation assay to quantify the P23H rhodopsin mutant transported on the plasma membrane. The robust and simple protocol of this HTS assay enabled us to explore the activities of about 79,000 small molecules for each screen. However, because this HTS assay reads luminescence signals, false positives including the β -gal inhibitors, colored or cytotoxic compounds are included in the hit list waiting to be identified by a secondary assay.

The traditional immunostaining and fluorescence imaging methods have been used for years to study the rhodopsin transport in mammalian cells^{5,14-16}. However, these conventional methods cannot be used to quantify pharmacological effects of more than 10 compounds towards rhodopsin transport because a reliable imaging analysis requires a large number of images taken under a highly consistent condition, which is not amendable by the conventional imaging methods. Here, we developed an immunostaining based high-content imaging protocol as a secondary assay to quantify the cell surface transport of misfolded rhodopsin mutants^{11,13,17}. To label rhodopsin on the plasma membrane, we skipped the step of cell membrane permeabilization and immunostained the rhodopsin mutants by a monoclonal (B6-30) anti-rhodopsin recognizing the N-terminal epitope of rhodopsin at the extracellular side of the cell membrane¹⁸. To visualize the mutant rhodopsin in the whole cell, we fused rhodopsin with the Venus fluorescence protein. By the quantification of the fluorescence intensities in different fluorescence channels, we are able to obtain multiple parameters from one single experiment including the total rhodopsin intensity in the whole cell, on the cell surface, and the ratio of rhodopsin fluorescence on the cell surface to that in the whole cell. Applying this method to stable cells expressing a total of six misfolded rhodopsin mutants, we can generate a pharmacological profile of multiple small molecule chaperones towards these mutants. In this

protocol, all cells are immunostained in a 384-well plate and imaged using an automated imaging system under a highly consistent imaging condition. An image analysis is performed to each well, containing images of more than 600 cells to reduce variation due to the heterogeneity of the cells with varying cell shape and protein expression level. The workflow of this protocol is summarized in **Figure 1**. The advantage of this method is that we obtain high-resolution images as well as multi-parameter quantifications from the image-based analysis. In general, this protocol can be modified and applied to quantify the transport of any misfolded membrane protein of interest.

PROTOCOLS:

Note: The rhodopsin transport assay.

1. Preparation and Culture of Cells

1.1. Revive cryo-preserved U2OS stable cells expressing the wild type (WT) or mutant mouse rhodopsin-Venus fusion proteins. Thaw the cells at 37 °C until only small ice crystals are left in the vial.

Note: The U2OS cells are used in this protocol because there is no photoreceptor cell line available for *in vitro* studies and the pre-ciliary biosynthesis of rhodopsin is regulated by similar molecular mechanisms in mammalian cells. Additionally, the U2OS cells attach tightly to the bottom of the plate and have large cell bodies, so they are ideal for the rhodopsin transport assay. Seven U2OS stable cells expressing the WT, T4R, P23H, P53R, C110Y, D190N and P267L rhodopsin mutants are used here as an example to show the quality and reliability of the assay. Stable cells expressing other rhodopsin mutants or other membrane proteins can be used, depending on the goal of the assay. Stable cells expressing human rhodopsin can be used in this assay if available. The mouse rhodopsin was used here because mouse and human rhodopsin proteins share 95% homology, and the compounds identified by this assay will be tested *in vivo* using a mouse adRP model carrying the rhodopsin P23H mutation⁸. The stable cells were generated as described previously¹⁹. The WT and mutant rhodopsin transcripts were quantified by q-PCR, and the clones of stable cells expressing similar levels of WT and mutant rhodopsin transcripts were selected for this assay. The expression of rhodopsin proteins was confirmed by immunoblot and immunostaining. The passage of cells used in this assay should be lower than 20.

1.2. Transfer each line of cells into a 15 mL conical tube containing 10 mL of growth medium (high glucose Dulbecco's modified Eagle's medium (DMEM) with 10% fetal bovine serum (FBS) and 5 µg/mL Plasmocin).

1.3. Centrifuge the tube at 200 x g for 5 min. Discard the supernatant and resuspend the cell pellet with 5 mL of cell growth medium for each cell line. Transfer each line of cell suspension into a 60 mm tissue culture dish and incubate at 37 °C with 5% CO₂.

1.4. Subculture the cells when the tissue culture dish reaches 90% confluence as described in reference¹².

2. Seeding Cells at 5,000 cells per Well

Note: Perform the following procedures in a tissue culture hood.

2.1. Treat the plate with poly-lysine.

2.1.1. One day before seeding the cells, treat a black-wall and clear bottom 384-well plate with 20 μ L/well of poly-lysine solution for 30 min.

2.1.2. Aspirate the liquid and allow all wells to dry for 1 h. Put back the plate lid and store the plate at 4 °C overnight for cell seeding.

2.2. Prepare the cell suspension.

2.2.1. Culture each cell line in growth medium in a 100 mm tissue culture dish until 90% confluence.

2.2.2. Wash each dish with phosphate buffered saline (PBS) and detach the cells with 1 mL of 0.05% Trypsin at room temperature.

2.2.3. Resuspend each line of cells in 10 mL of assay medium (high-glucose DMEM with 10% FBS, 100 units/mL penicillin and 100 μ g/mL streptomycin).

2.2.4. Count the cells and dilute each line of cells to 1.25×10^4 cells/mL with the assay medium.

2.3. Seed the cells.

2.3.1. Use an electronic multichannel pipette or an automated reagent dispenser to dispense 40 μ L/well of the cell suspension to three columns per cell line and fill columns 1-21 of the 384-well plate (**Figure 2**).

2.3.2. Add 40 μ L/well of U2OS (P23H-Rhodopsin-Venus) to columns 22-23 and 40 μ L/well of U2OS (Rhodopsin-Venus) to column 24, as controls.

2.3.3. Centrifuge the plate at 300 x g for 30 s to bring down all cells to the bottom of the 384-well plate.

Note: Avoid physical shock to the plate after cell seeding. Otherwise, cells will be crushed to one corner of each well, and the plate will not be suitable for high-content imaging.

2.3.4. Incubate the 384-well plate at 37 °C with 5% CO₂ for 3 h for the cells to attach to the bottom of the plate.

3. Treating the Cells with Compounds

3.1. Generate a plate map with treatment conditions as shown in **Figure 2**.

3.2. Prepare 300 μ L of 5x working solutions of up to 15 compounds in a 96-well plate.

3.2.1. Dilute cps 1 to 15 with the assay medium to five times of their final concentrations in wells A1 to G2 of the 96-well plate (**Figure 2A**). Add 300 μ L of assay medium in well H2.

Note: The final concentration of each compound is used at the most effective concentration for rescuing the transport of the P23H rhodopsin by the HTS^{12,13}.

3.2.2. Add 100 μ L per well of 2% dimethyl sulfoxide (DMSO) and 25 μ M 9-*cis*-retinal that are diluted in the assay medium to columns 11 and 12, respectively. Add 9-*cis*-retinal in dim light.

3.3. Adding 10 μ L per well of 5x working solutions to the 384-well plate cultured with the cells (**Figure 2B**).

3.3.1. Use an electronic multi-channel pipette to add compounds 1, 3, 5, 7, 9, 11, 13, and 15 to rows A, C, E, G, I, K, M, and O from columns 1 to 21 (**Figure 2**). Add compounds 2, 4, 6, 8, 10, 12, 14 and M to rows B, D, F, H, J, L, N, and P from columns 1 to 21.

3.3.2. Add 10 μ L per well of 2% DMSO to columns 22 and 24. Add 10 μ L per well of 25 μ M 9-*cis*-retinal to column 23.

Note: DMSO is used as a vehicle control because all the compounds are initially dissolved in DMSO as stocks. Column 22 containing DMSO treated cells expressing the P23H rhodopsin is used as the 0% control. 9-*Cis*-retinal treated cells expressing the P23H rhodopsin is used as the 100% control.

3.4. Cover the 384-well plate with aluminum foil and incubate the plate at 37 °C for 24 h.

4. Immunostaining without Membrane Permeabilization to Stain Rhodopsin Protein on the Cell Surface.

Note: Avoid any detergent in the entire immunostaining process to keep cell membrane intact.

4.1. Prepare 4% paraformaldehyde (PFA) by diluting the 16% PFA with PBS in a 1:4 volume ratio in a chemical fume hood. Transfer the 4% PFA in a reagent reservoir.

4.2. Take out the 384-well plate in a dark room with dim red light. Use an 8-channel aspirator connected to a vacuum collection bottle to gently aspirate the medium. Use an electronic multichannel pipette to add 20 μ L per well of freshly prepared 4% PFA to the entire 384-well plate and incubate for 20 min at room temperature. To avoid cell detachment, always point the

tips of the aspirator to the same side of each well during aspirations. Do not touch the middle bottom area of each well. When taking images, select fields to avoid the region touched by the aspirator. For incubations longer than 10 min, cover the 384-well plate with its lid to avoid evaporation.

Note: Cells are fixed in a dark room to avoid photobleaching of the regenerated isorhodopsin that will affect the result of the 100% control. After fixation, the 384-well plate can be taken out under normal light.

4.3. Use an 8-channel aspirator to aspirate the PFA in each well and use an electronic multi-channel pipette to add 50 μL per well of PBS. Repeat two more times to perform three washes with PBS.

Caution: The waste liquid containing PFA are collected in a capped bottle and is to be disposed of as a hazardous chemical waste after the experiment.

4.4. Block the cells by adding 20 μL per well of 5% goat serum to the entire 384-well plate and incubate at room temperature for 30 min.

4.5. Aspirate the 5% goat serum and add 15 μL per well of 20 $\mu\text{g mL}^{-1}$ B6-30 anti-rhodopsin antibody in 1% goat serum to rows A to O. Add 15 μL per well of 1% goat serum to row P for the secondary antibody-only control group.

4.6. Incubate the 384-well plate at room temperature for 90 min or at 4 $^{\circ}\text{C}$ overnight. Cover the 384-well plate with aluminum foil to avoid photobleaching of the fluorophores.

4.7. Wash the plate 3 times with 50 μL per well of PBS.

4.8. Aspirate PBS and add 15 μL per well of 5 $\mu\text{g mL}^{-1}$ Cy3-conjugated goat anti-mouse IgG antibody. Cover the 384-well plate with aluminum foil and incubate at room temperature for 1 h or at 4 $^{\circ}\text{C}$ overnight.

4.9. Wash the plate 3 times with 50 μL per well of PBS. Add 50 μL per well of PBS containing 1 $\mu\text{g mL}^{-1}$ Hoechst 33342 to stain nuclei at room temperature for 15 min.

4.10. Seal the 384-well plate with a transparent film before imaging. Cover the 384-well plate with aluminum foil and store at 4 $^{\circ}\text{C}$ for up to a week if images are taken immediately.

5. Imaging.

Note: This high-content imaging procedure is adapted to the imaging system listed in the **Table of Material**. Procedures can be different if using other high-content imaging systems.

5.1. Remove the lid and put the 384-well plate into the high-content imager with A1

positioned on the top left corner of the plate.

5.2. Open the image acquisition software to set up parameters for image acquisition.

5.2.1. Open the Plate Acquisition Setup window and create new setting or load an existing setup file.

5.2.2. Select the 20X objective and set up pixel binning as 2 so the calibrated pixel size is $0.80 \times 0.80 \mu\text{m}$. Set the scan lines as 2000 and the image size (W X H) as 1000 X 1000 pixels ($800.00 \times 800.00 \mu\text{m}$) per site.

5.2.3. Select the plate type to be imaged. Use the information provided by the manufacturer of the 384-well plate to fill in the plate dimensions.

5.2.4. Select the wells to be imaged for the 384-well plate.

5.2.5. Select four sites to be imaged per well. Avoid the side of the well touched by the aspiration tips.

5.2.6. Select excitation lasers as 405, 488 and 561 nm. Select emission filters for DAPI, FITC and Texas Red channels. Optimize the laser power and gains of each channel to ensure the brightness of images taken from the positive control wells are less than the saturation threshold.

5.2.7. Select well-to-well focus for autofocus. Select the first well acquired as the initial well for finding samples. Set site autofocus to all sites.

5.2.8. Select four averages per line for each channel. Optimize the Z-offset value for each channel.

5.2.9. Test 2-3 wells at the diagonal corners of the 384 well plate to make sure the images are on focus for all tested wells, images from all sites per well have cells with more than 40% confluence, and fluorescence intensities of all channels are about half saturated in the 100% control wells.

5.2.10. Save the image acquisition method.

5.3. Run the entire plate. Watch the imager until it finishes capturing images from the first column of the plate to double-check the image quality before leaving the imager. Take the 384-well plate out and store at 4°C for future use.

Note: Depending on the number of sites selected per well and the channels taken, it takes 40 min to 3 h to finish imaging one 384-well plate.

6. Image Analysis.

6.1. Pull out the image data using a high-content image analysis software. Select one of the 100% control wells (column 23) to set up parameters.

6.2. Select the **Multi-Wavelength Cell Scoring** as the analysis method and start configuring settings.

6.2.1. Define the nuclei using images from the DAPI channel. Preview to make sure the defined nuclei shapes in the selected well fits well with the nuclei images.

6.2.2. Define the shape of cell in the FITC channel where rhodopsin-Venus is imaged.

6.2.3. Define the rhodopsin cell surface stain areas in the Texas Red channel.

6.2.4. Test the current algorithm in 5 wells to determine if the settings are optimized. Save the settings and close the **Configuration** window.

6.3. Run all the wells with the optimized analysis method.

6.4. Export **Object Number** as intact cell number. Export the **Average Intensity** of the FITC channel as Rhodopsin-Venus Intensity (Rhodopsin-Venus INT). Export the **Average Intensity** of the Texas Red channel as rhodopsin intensity on the cell surface (Rhodopsin INT on the cell surface).

6.5. Open the exported data in a spreadsheet software. Divide the rhodopsin intensity on the cell surface by the rhodopsin-Venus INT as MEM-to-total ratio. Calculate the Z'-factors for each parameter to evaluate the assay quality. $Z' = 1 - 3 \times (\text{STD}_{100\% \text{ control}} + \text{STD}_{0\% \text{ control}}) / |\text{Mean}_{100\% \text{ control}} - \text{Mean}_{0\% \text{ control}}|$.

Note: A Z'-factor higher than 0 indicates a moderate assay sufficient for a high-content screen, and a Z' factor between 0.5 and 1 suggests an outstanding assay required for a high-throughput screen^{20,21}.

6.6. Use the spreadsheet software to generate a two-color heat map for each parameter. Arrange the name of cell lines on the X-axis and the compounds on the Y-axis.

REPRESENTATIVE RESULTS:

We characterized the rhodopsin transport with three parameters: the rhodopsin-Venus intensity in the whole cell (Rhodopsin-Venus INT), the immunostaining intensity of rhodopsin on the plasma membrane (Rhodopsin INT on the cell surface), and the ratio of rhodopsin stain on the cell surface to rhodopsin-Venus intensity in the whole cell (MEM-Total Ratio). A representative result of the rhodopsin transport assay is shown in **Figures 3** and **4**. Using DMSO and 9-*cis*-retinal treated cells expressing the P23H-rhodopsin-Venus as the 0 and 100% controls, respectively, the Z'-factors for these three parameters are in the range between 0 to 0.5, suggesting that the assay

has moderate quality, sufficient for high-content imaging²¹. Even though the optimized Z'-factors are lower than 0.5 due to its relatively complex procedures compared to a HTS assay, this assay is still robust and reliable for an image-based analysis. An active compound that rescues a misfolded rhodopsin should show higher values of Rhodopsin INT on the cell surface and MEM-Total Ratio than DMSO, with a *P* value lower than 0.05. Three 2-D heat maps were generated from these three parameters to compare the average rhodopsin amount and localization per cell (**Figure 4**). Repeated in triplicates, WT and six rhodopsin mutants are listed horizontally, and the effects of compound treatments are compared vertically. In agreement with previous studies, the rhodopsin INT on the cell surface and the MEM-Total ratio of are lower for the six mutants compared to the WT rhodopsin treated with DMSO (**Figure 4C**)^{5,22,23}. The rhodopsin INT on the cell surface and its MEM-to-Total ratio are increased by 9-*cis*-retinal treatment for the T4R, P23H, D190N and P267L, but not the P53R or C110Y mutants, suggesting that 9-*cis*-retinal rescues the transport of the T4R, P23H, D190N and P267L rhodopsin mutants. All the cps showed varying levels of increase in the Rhodopsin INT on the cell surface for the T4R, P23H and D190N. Cps 3, 4, 5, 7, 8 and 11 increased the rhodopsin-Venus INT but not the MEM-to-Total ratio of these rhodopsin mutants, suggesting that these compounds only increased the rhodopsin amount. Cps 1, 2 6 and 9 significantly increased the MEM-to-Total ratio of T4R, P23H, D190N and P267L rhodopsin mutants, suggesting that these compounds rescue the transport of these rhodopsin mutants to the plasma membrane. The 2-D profiles provide a comprehensive overview of rhodopsin transport affected by these adRP associated mutations that are mitigated by different pharmacological treatment.

FIGURE AND TABLE LEGENDS

Figure 1. The workflow of the rhodopsin transport assay. Procedures for cell surface staining of rhodopsin without membrane permeabilization for the rhodopsin transport assay.

Figure 2. Illustrations for the preparation of 5x working solutions and the liquid transfer from the 96-well plate to the 384-well plate. (A) The 96-well plate layout of the 5x working solutions. Wells A1 to G2 have 300 μ L per well of up to 15 5x working solutions and assay medium (M) as illustrated in columns 1 and 2. Compounds 14 and 15 are 2% DMSO and 25 μ M 9-*cis*-retinal, respectively, for the treatment to the seven cell lines expressing WT and mutant rhodopsin. Additionally, columns 11 and 12 have 100 μ L per well of 2% DMSO and 25 μ M 9-*cis*-retinal controls, respectively, treated to the cells expressing the P23H rhodopsin for the calculation of Z'-factors. (B) The 384-well plate layout for cell type and treatment conditions. The U2OS cells expressing the WT, T4R, P23H, P53R, C110Y, D190N and P267L rhodopsin-Venus are seeded as illustrated. Treatment conditions are labeled in blue. Pink and blue tips demonstrate the well-to-well liquid transfer from the 96-well plate to the 384 plate using a multichannel pipette.

Figure 3. Representative images and quantifications for the controls of the rhodopsin transport assay. (A) Venus fluorescence (green) and cell surface immunostaining (red) of U2OS cells expressing WT or P23H rhodopsin-Venus treated with DMSO or 5 μ M 9-*cis*-retinal. Scale bar = 200 μ m. (B) A column plot of mean Venus intensity per cell representing rhodopsin amount in the whole cell (Rhodopsin-Venus INT). *****p*<0.0001. Z'-factor is shown under the black line. Column value and error bar are average and standard deviation (S.D.) of 16 replicates,

respectively. (C) A column plot of mean Cy3 intensity per cell representing the rhodopsin stained on the cell surface (Rhodopsin INT on the cell surface). (D) A column plot of the ratio of mean cy3 intensity per cell to mean Venus intensity per cell representing the ratio of rhodopsin level on the cell surface to its whole-cell level (MEM-to-total ratio).

Figure 4. A representative high-content analysis of the rhodopsin transport assay shown as 2-color heat maps. (A) The heat map of mean Venus intensity per cell representing the whole-cell rhodopsin level (Rhodopsin-Venus INT). Each block represents a data point and each condition was tested in triplicate. The color legend is shown on the left. Cp, compound. (B) The heat map of mean Cy3 intensity per cell representing the rhodopsin stained on the cell surface (Rhodopsin INT on the cell surface). (C) The heat map of the mean Cy3 intensity per cell to the mean Venus intensity per cell representing the ratio of rhodopsin level on the cell surface to its whole-cell level (MEM-to-total ratio).

DISCUSSION:

Here, we showed a high-content imaging assay used for characterizing hits identified from a HTS. The only automation involved in these protocols is the high-content imager. The immunostaining and fluorescence imaging of rhodopsin have been used commonly to characterize the localization of rhodopsin^{5,14-16}. However, the quantification of images taken by the traditional imaging methods is limited by the lack of sufficient cell images per condition, low capacity of images per experiment, and lack of a quality control parameter. We adapted the traditional immunostaining protocol to the 384-well format and replaced the traditional imaging with high-content imaging. Using this high-content imaging protocol, we successfully selected and characterized the activities of hits identified by a HTS^{11,13,17}. Compared to the traditional immunostaining and imaging methods, this protocol significantly increased the consistence of imaging conditions, imaging capacity, and image analysis power, which enabled us to quantitatively compare the pharmacological effects of 11 compounds towards the transport of six adRP associated rhodopsin mutants.

The major changes of this protocol compared to the previously used protocols for rhodopsin immunostaining and imaging are: (1) growing and immunostaining cells in a clear-bottom 384-well plate; (2) imaging cells using a high-content imager; and (3) analyzing data with a high-content image analysis software. Due to these changes, an initial optimization is required to find the best cell seeding number, antibody concentrations, imaging conditions, and image analysis algorithms.

The critical steps of the protocol include: (1) seeding cells that allow 50-70% confluence before fixation; (2) careful aspirations to avoid cell detachment; (2) imaging several wells across the whole plate to make sure images are on focus and fluoresce of all channels does not exceed half of the threshold of the imager for the positive control wells before imaging the whole plate; and (3) keeping the Z'-factor higher than 0 to ensure the reliability of the assay.

The most common problems that could be encountered for this protocol are cell detachment and low Z'-factors. To avoid the first issue, pretreat the 384-well plate with poly-L-lysine to facilitate

the cell attachment and avoid using cell lines that detach easily such as the Hek293 cells. Additionally, limit the aspiration tip to touch only one side of each well during aspiration and select the other side of each well for imaging. To improve the Z'-factor and the assay quality, optimize the cell seeding number and image analysis parameters to make sure the cell shape or nuclei shape defined by the software fits well with each object in each fluorescence channel.

Compared to other methods to quantify rhodopsin transport, such as a cell surface ELISA, or a β -galactosidase fragment complementation assay, which calculate the target protein level on the cell surface in all cells, this high-content imaging method quantifies average protein level per cell; and, this unique feature avoids a critical variation factor, cell number that affects the final readouts in other methods. Additionally, due to the large number of cells imaged and quantified by the high-content imaging method, the parameters averaged from all cells per well showed low variation between replicates, thus adding to the reliability of the assay.

One limitation of this protocol is that they are not the best assays for HTS, due to its relatively complicated procedure and the 2 h per plate imaging time. Thus, we recommend alternative reporter assays for screening large small-molecule libraries with more than 5,000 compounds, and use this high-content imaging protocol for focused characterization assays limited to less than 100 compounds. The second limitation of this protocol is its lack of standards to show whether the Venus fluorescence or the immunostaining fluorescence intensities are in a linear correlation with the quantity of rhodopsin protein amount per cell. To avoid saturation by immunostaining, we recommend testing and plotting the immunostaining intensities of the cells incubated with different concentrations of primary and secondary antibodies. Select the antibody concentrations within the linear range of fluorescence change.

Expanding from the current application, we will quantify rhodopsin transport from images of cells transiently transfected with 28 different rhodopsin mutants under treatment with up to 10 compounds to generate a pharmacological database of these compounds' activity for guidance of potential treatments to adRP patients carrying these rhodopsin mutations. This protocol can also be easily adapted to the translocation assays of any membrane protein of interest that will be useful for drug discoveries of other protein misfolding diseases.

ACKNOWLEDGMENTS:

We thank Dr. Mark E. Schurdak and University of Pittsburgh Drug Discovery Institute for providing the high-content imager and initial trainings. Dr. Krzysztof Palczewski (Case Western Reserve University) generously shared the 1D4 and B630 anti-rhodopsin antibodies and the NIH3T3(Rhodopsin/GFP) and NIH3T3(P23H-rhodopsin/GFP) cells. The plasmid containing the cDNA of mouse rhodopsin-Venus construct was shared by Dr. Nevin Lambert (Augusta University). This work was supported by the National Institute of Health grant EY024992 to YC and P30EY008098 from University of Pittsburgh Vision Research Core grant.

DISCLOSURES:

The authors have nothing to disclose.

REFERENCES:

- 1 Gregersen, N., Bross, P., Vang, S. & Christensen, J. H. Protein misfolding and human disease. *Annual Review of Genomics and Human Genetics*. **7** 103-124, (2006).
- 2 Daiger, S. P., Bowne, S. J. & Sullivan, L. S. Perspective on genes and mutations causing retinitis pigmentosa. *Archives of Ophthalmology*. **125** (2), 151-158, (2007).
- 3 Daiger, S. P., Sullivan, L. S. & Bowne, S. J. Genes and mutations causing retinitis pigmentosa. *Clinical Genetics*. **84** (2), 132-141, (2013).
- 4 Stenson, P. D. *et al.* The Human Gene Mutation Database: towards a comprehensive repository of inherited mutation data for medical research, genetic diagnosis and next-generation sequencing studies. *Human Genetics*. **136** (6), 665-677, (2017).
- 5 Sung, C. H., Schneider, B. G., Agarwal, N., Papermaster, D. S. & Nathans, J. Functional heterogeneity of mutant rhodopsins responsible for autosomal dominant retinitis pigmentosa. *Proceedings of the National Academy of Sciences of the United States of America*. **88** (19), 8840-8844, (1991).
- 6 Athanasiou, D. *et al.* The molecular and cellular basis of rhodopsin retinitis pigmentosa reveals potential strategies for therapy. *Progress in Retinal and Eye Research*. **62** 1-23, (2018).
- 7 Chiang, W. C. *et al.* Robust Endoplasmic Reticulum-Associated Degradation of Rhodopsin Precedes Retinal Degeneration. *Molecular Neurobiology*. **52** (1), 679-695, (2015).
- 8 Sakami, S. *et al.* Probing mechanisms of photoreceptor degeneration in a new mouse model of the common form of autosomal dominant retinitis pigmentosa due to P23H opsin mutations. *Journal of Biological Chemistry*. **286** (12), 10551-10567, (2011).
- 9 Dryja, T. P. *et al.* Mutations within the rhodopsin gene in patients with autosomal dominant retinitis pigmentosa. *New England Journal of Medicine*. **323** (19), 1302-1307, (1990).
- 10 Sohocki, M. M. *et al.* Prevalence of mutations causing retinitis pigmentosa and other inherited retinopathies. *Human Mutation*. **17** (1), 42-51, (2001).
- 11 Chen, Y. *et al.* A novel small molecule chaperone of rod opsin and its potential therapy for retinal degeneration. *Nature Communications*. **9** (1), 1976, (2018).
- 12 Chen, Y. & Tang, H. High-throughput screening assays to identify small molecules preventing photoreceptor degeneration caused by the rhodopsin P23H mutation. *Methods in Molecular Biology*. **1271** 369-390, (2015).
- 13 Chen, Y. *et al.* A High-Throughput Drug Screening Strategy for Detecting Rhodopsin P23H Mutant Rescue and Degradation. *Investigative Ophthalmology & Visual Science*. **56** (4), 2553-2567, (2015).
- 14 Noorwez, S. M. *et al.* Pharmacological chaperone-mediated in vivo folding and stabilization of the P23H-opsin mutant associated with autosomal dominant retinitis pigmentosa. *Journal of Biological Chemistry*. **278** (16), 14442-14450, (2003).
- 15 Saliba, R. S., Munro, P. M., Luthert, P. J. & Cheetham, M. E. The cellular fate of mutant rhodopsin: quality control, degradation and aggresome formation. *Journal of Cell Science*. **115** (Pt 14), 2907-2918, (2002).
- 16 Kaushal, S. & Khorana, H. G. Structure and function in rhodopsin. 7. Point mutations associated with autosomal dominant retinitis pigmentosa. *Biochemistry*. **33** (20), 6121-6128, (1994).

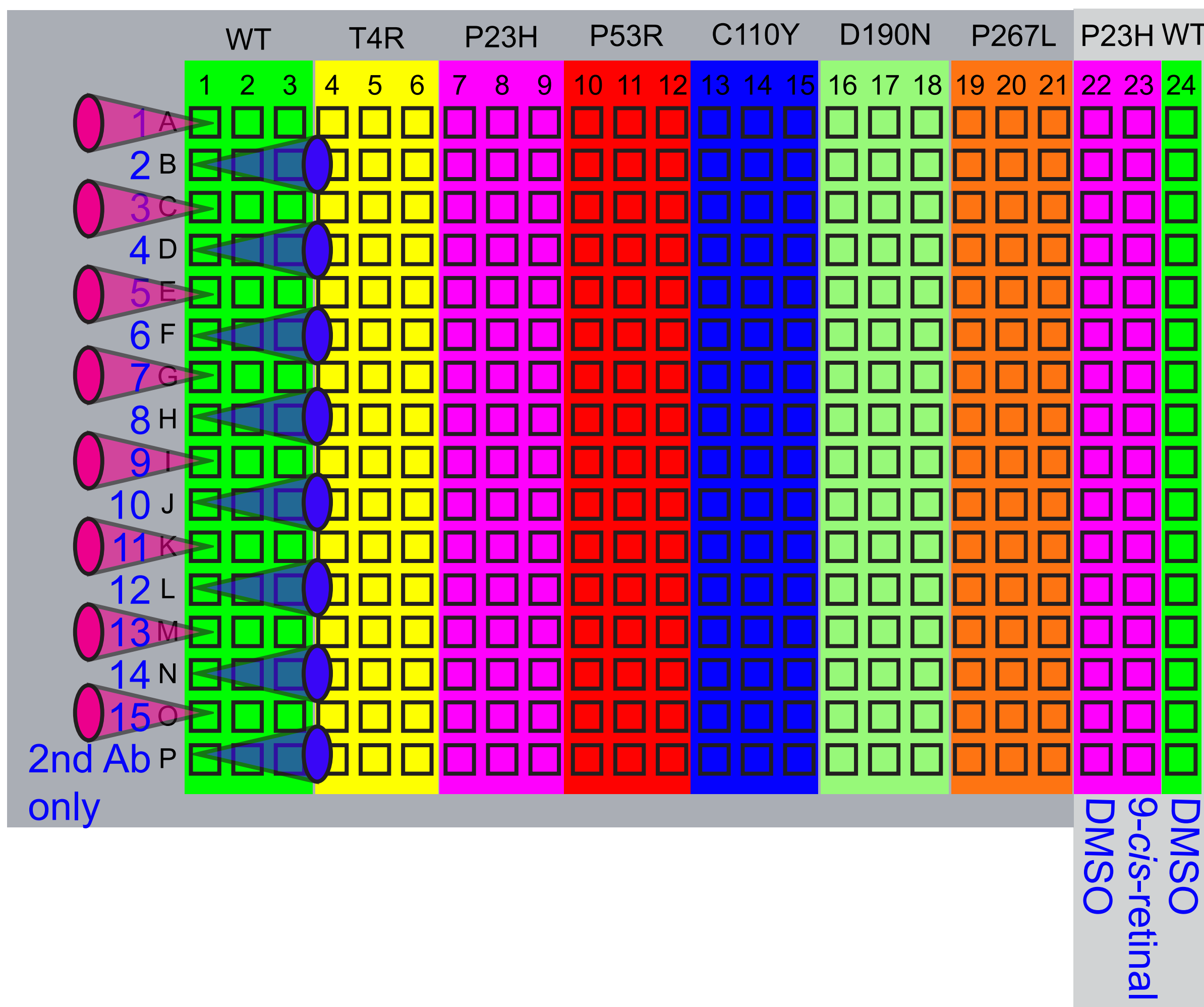
529 17 Chen, Y., Brooks, M. J., Gieser, L., Swaroop, A. & Palczewski, K. Transcriptome profiling of
 530 NIH3T3 cell lines expressing opsin and the P23H opsin mutant identifies candidate drugs
 531 for the treatment of retinitis pigmentosa. *Pharmacological Research*. **115** 1-13, (2016).
 532 18 Adamus, G. *et al.* Anti-rhodopsin monoclonal antibodies of defined specificity:
 533 characterization and application. *Vision Research*. **31** (1), 17-31, (1991).
 534 19 Goodson, H. V., Dzurisin, J. S. & Wadsworth, P. Generation of stable cell lines expressing
 535 GFP-tubulin and photoactivatable-GFP-tubulin and characterization of clones. *Cold Spring*
 536 *Harbor Protocols*. **2010** (9), pdb prot5480, (2010).
 537 20 Zhang, J. H., Chung, T. D. & Oldenburg, K. R. A Simple Statistical Parameter for Use in
 538 Evaluation and Validation of High Throughput Screening Assays. *Journal of Biomolecular*
 539 *Screening*. **4** (2), 67-73, (1999).
 540 21 Bray, M. A. & Carpenter, A. Advanced Assay Development Guidelines for Image-Based
 541 High Content Screening and Analysis. In *Assay Guidance Manual* eds Sittampalam G. S. *et*
 542 *al.* Bethesda (MD): Eli Lilly & Company and the National Center for Advancing
 543 Translational Sciences (2004).
 544 22 Sung, C. H., Davenport, C. M. & Nathans, J. Rhodopsin mutations responsible for
 545 autosomal dominant retinitis pigmentosa. Clustering of functional classes along the
 546 polypeptide chain. *Journal of Biological Chemistry*. **268** (35), 26645-26649, (1993).
 547 23 Krebs, M. P. *et al.* Molecular mechanisms of rhodopsin retinitis pigmentosa and the
 548 efficacy of pharmacological rescue. *Journal of Molecular Biology*. **395** (5), 1063-1078,
 549 (2010).
 550
 551

| | |
|---|--------|
| Day 1: Cell seeding and attachment | 2 h |
| Day 1: Compound treatment | 24 h |
| Day 2: Immunostaining | 4-5 h |
| Fix cells with 4 % PFA | 20 min |
| Wash 3 times with PBS | 20 min |
| Block cells with 5 % goat serum | 30 min |
| Incubate with 20 mg/mL B6-30 anti-rhodopsin antibody | 1 h |
| Wash 3 times with PBS | 20 min |
| Incubate with 2 mg/mL Cy3-conjugated goat anti-mouse IgG secondary antibody | 1 h |
| Wash 3 times with PBS | 20 min |
| Incubate with PBS with 1 ug/mL Hoescht 33342 | 15 min |
| Day 2: Imaging | 2 h |
| Day 2: Data analysis | 6 h |

15: DMSO

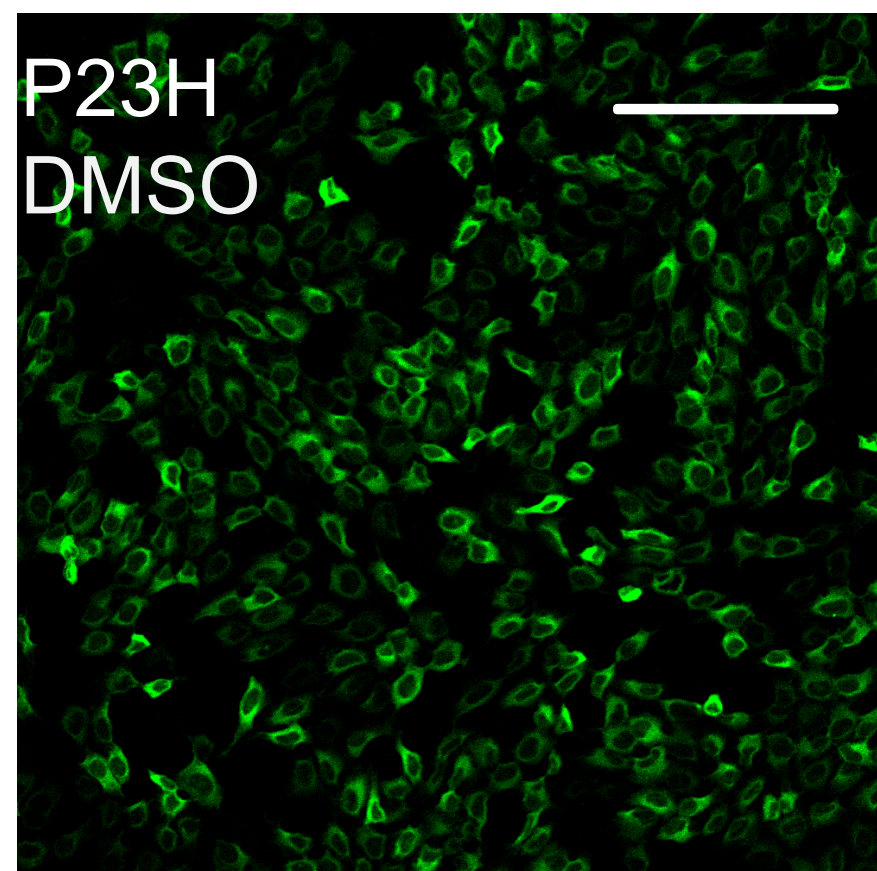


15: DMSO

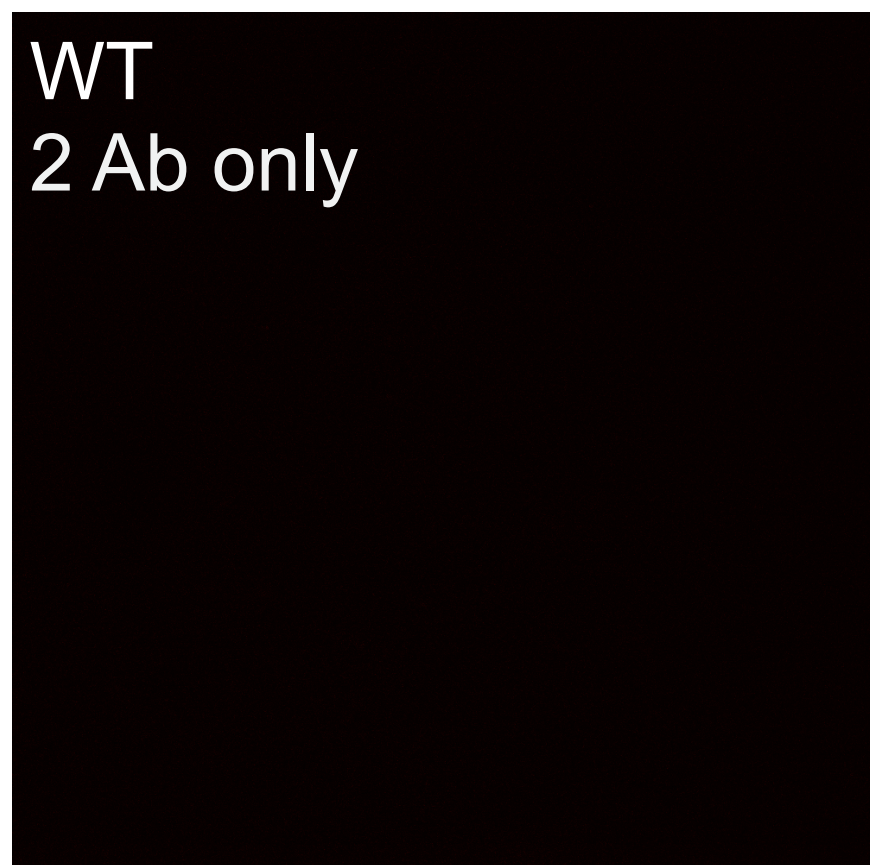
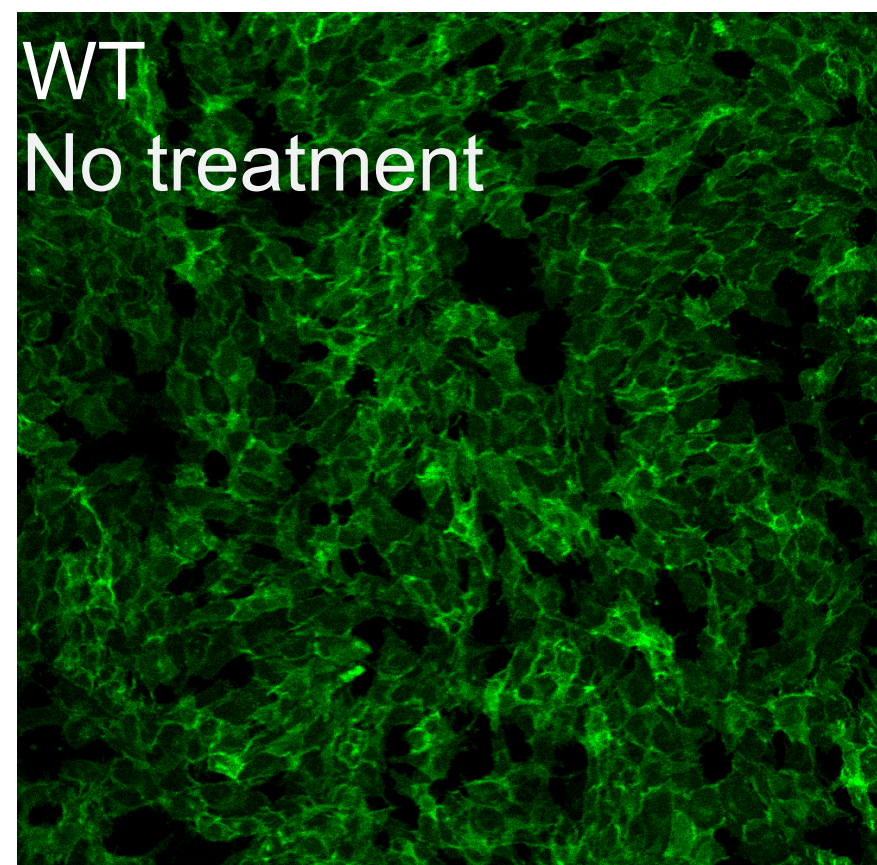
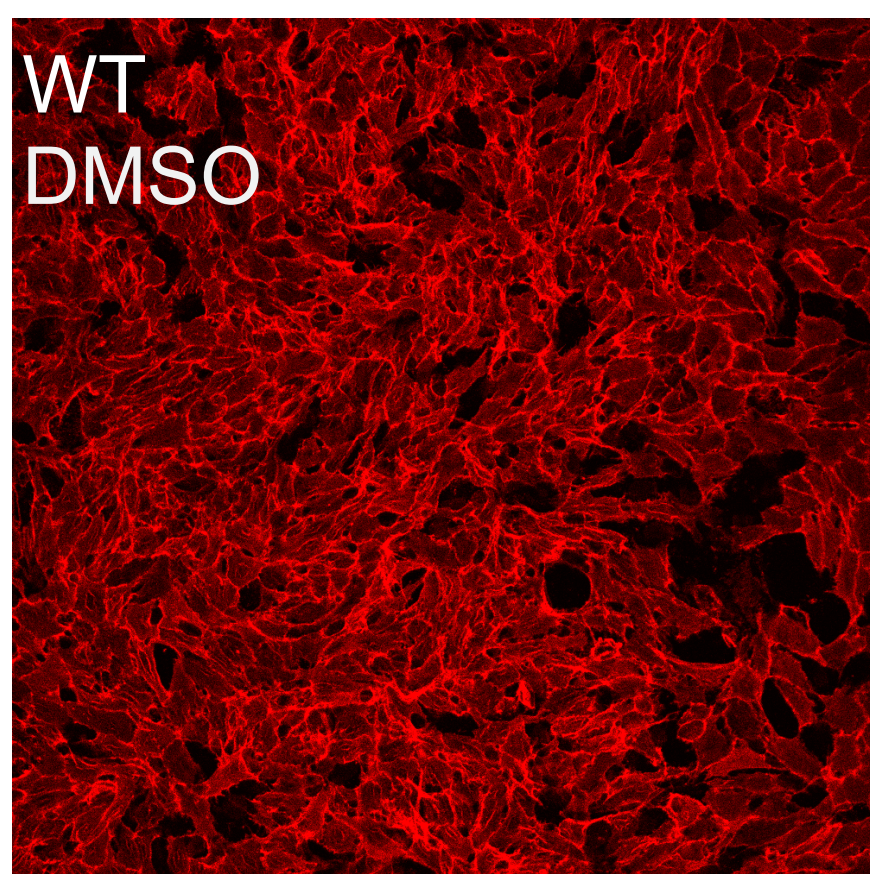
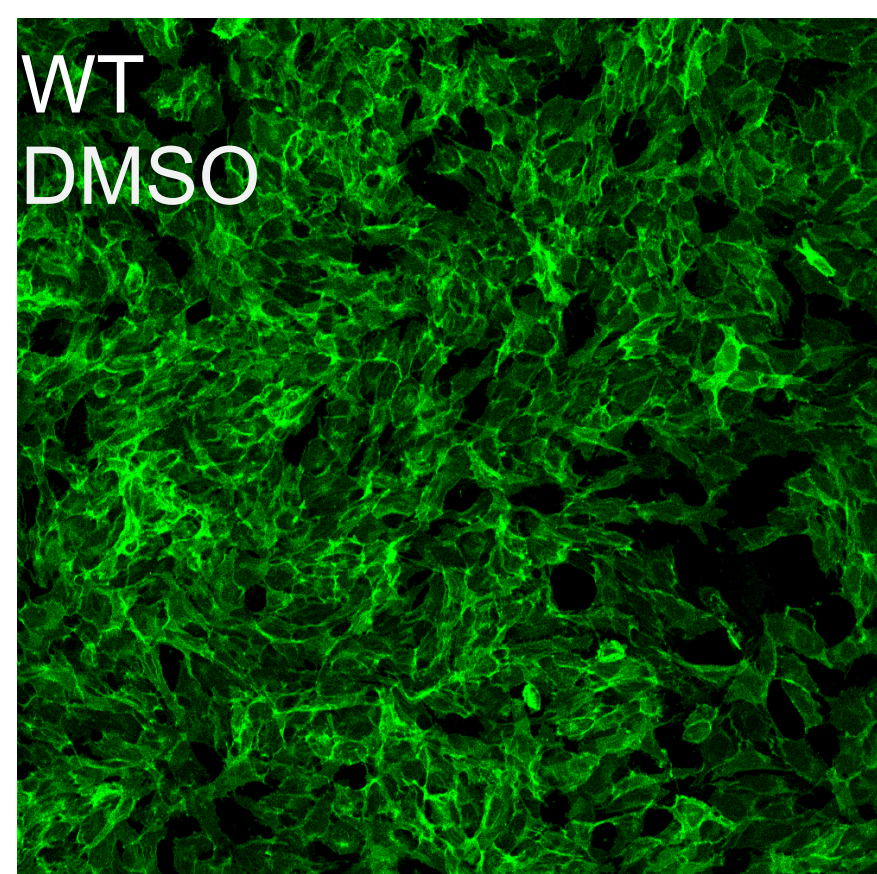
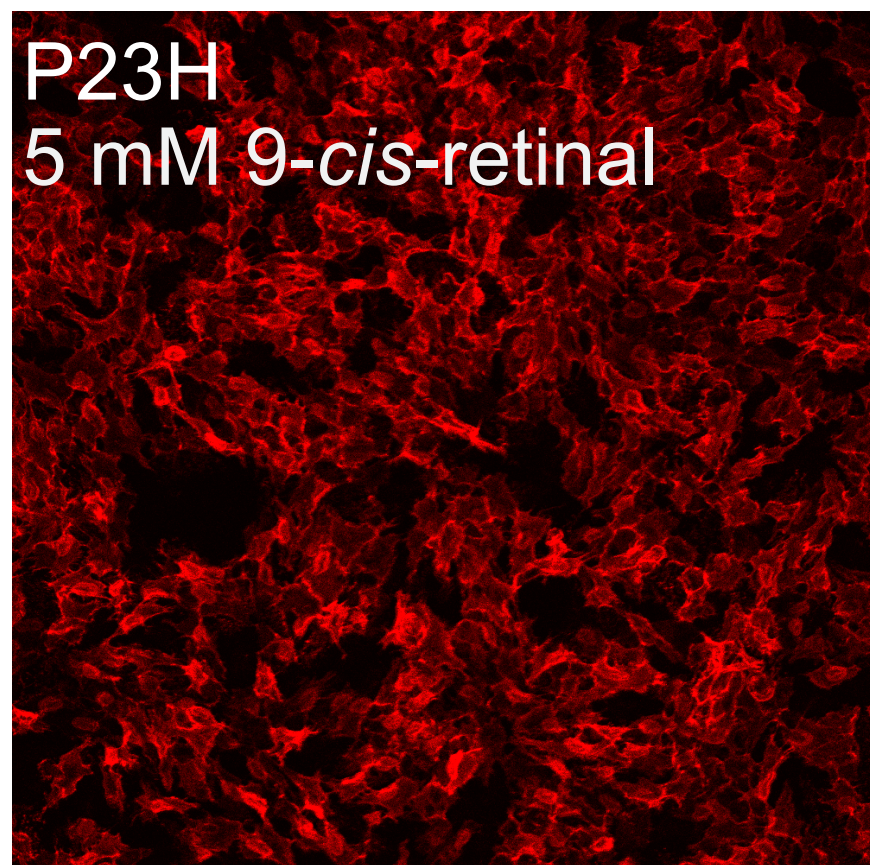
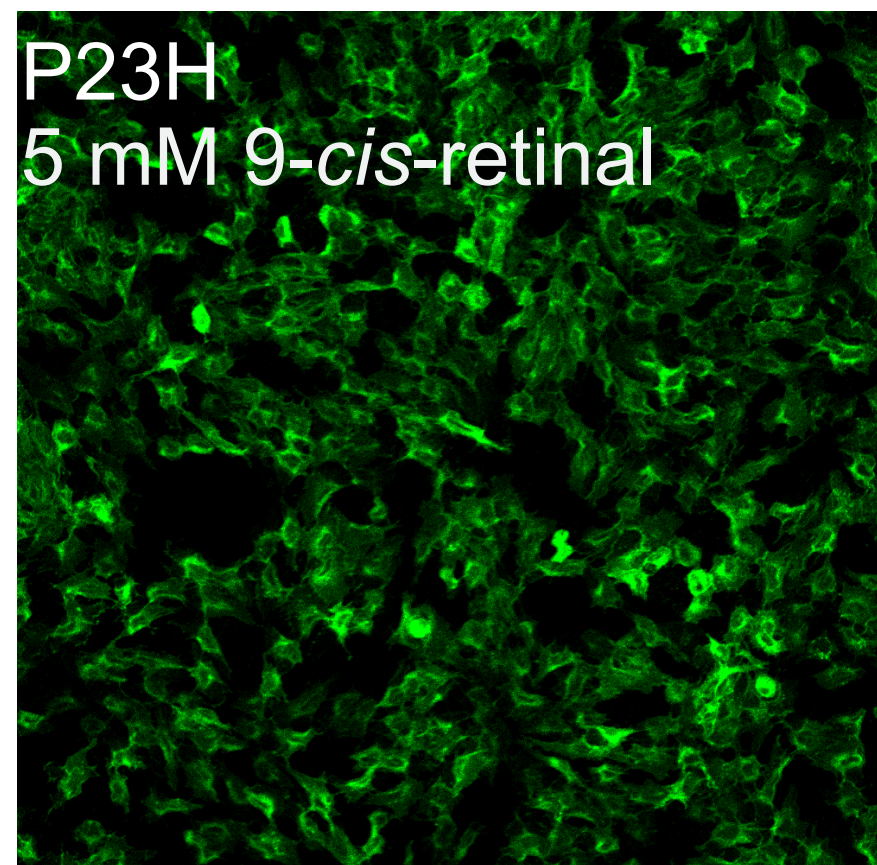
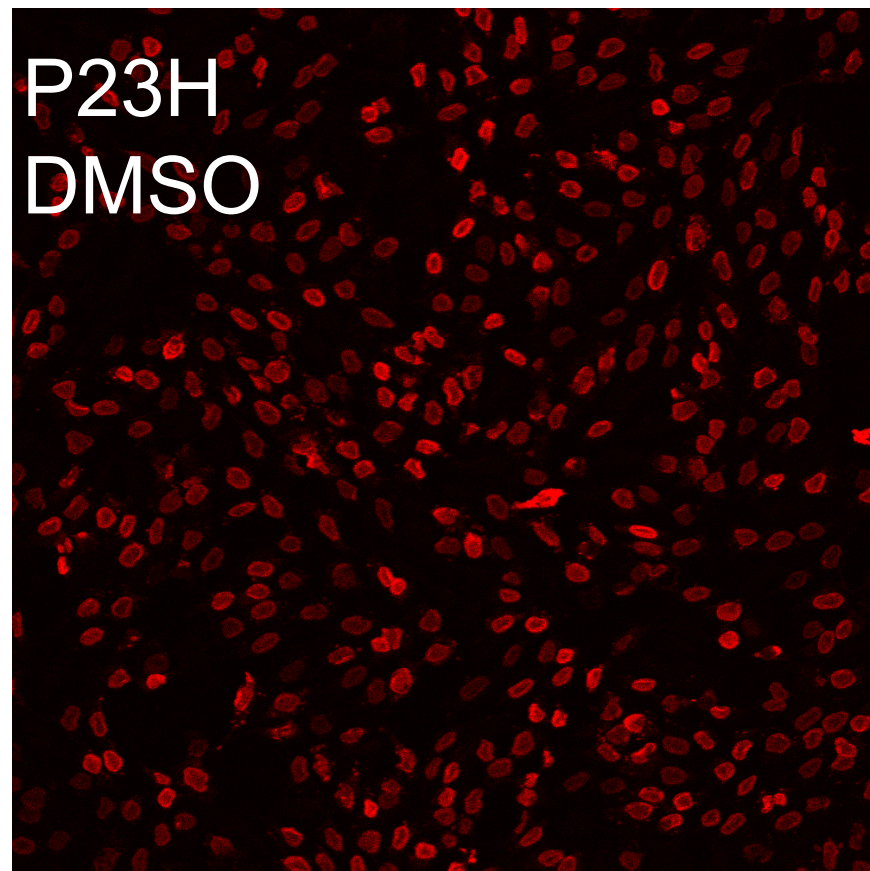


A

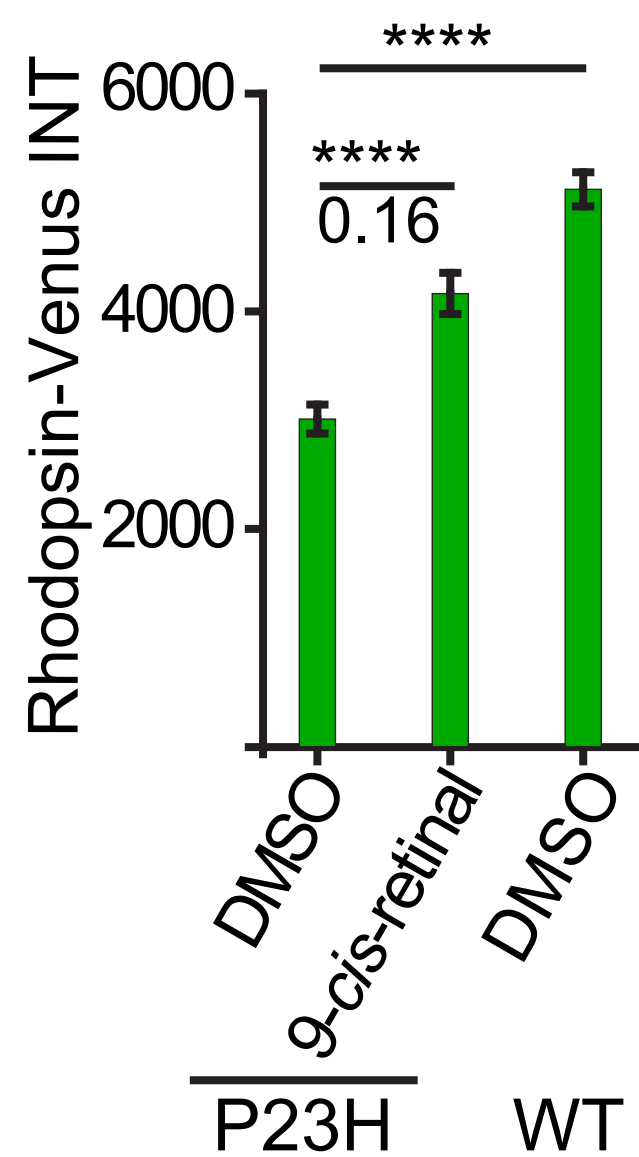
Venus



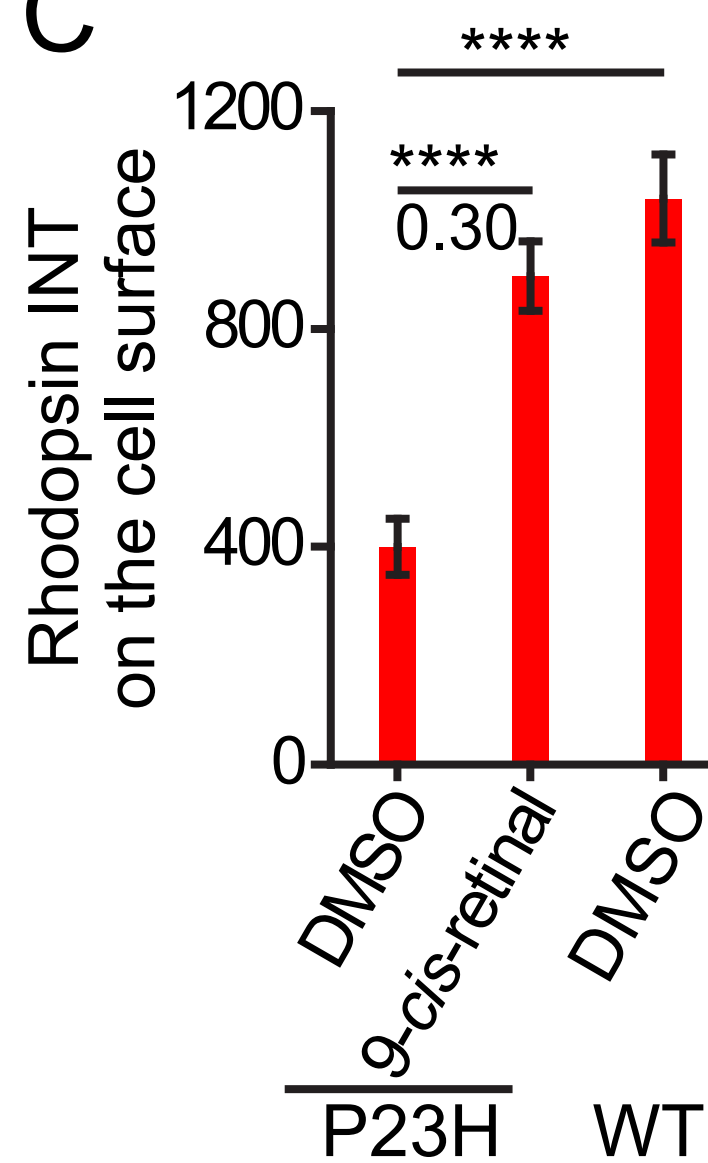
Cell surface stain



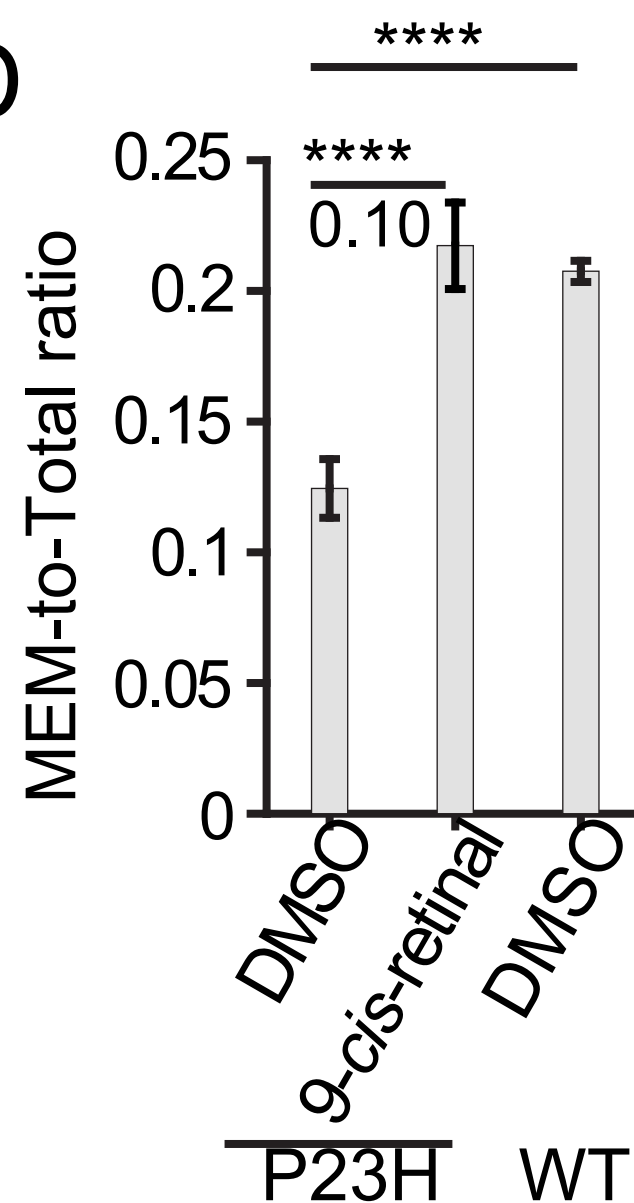
B



C

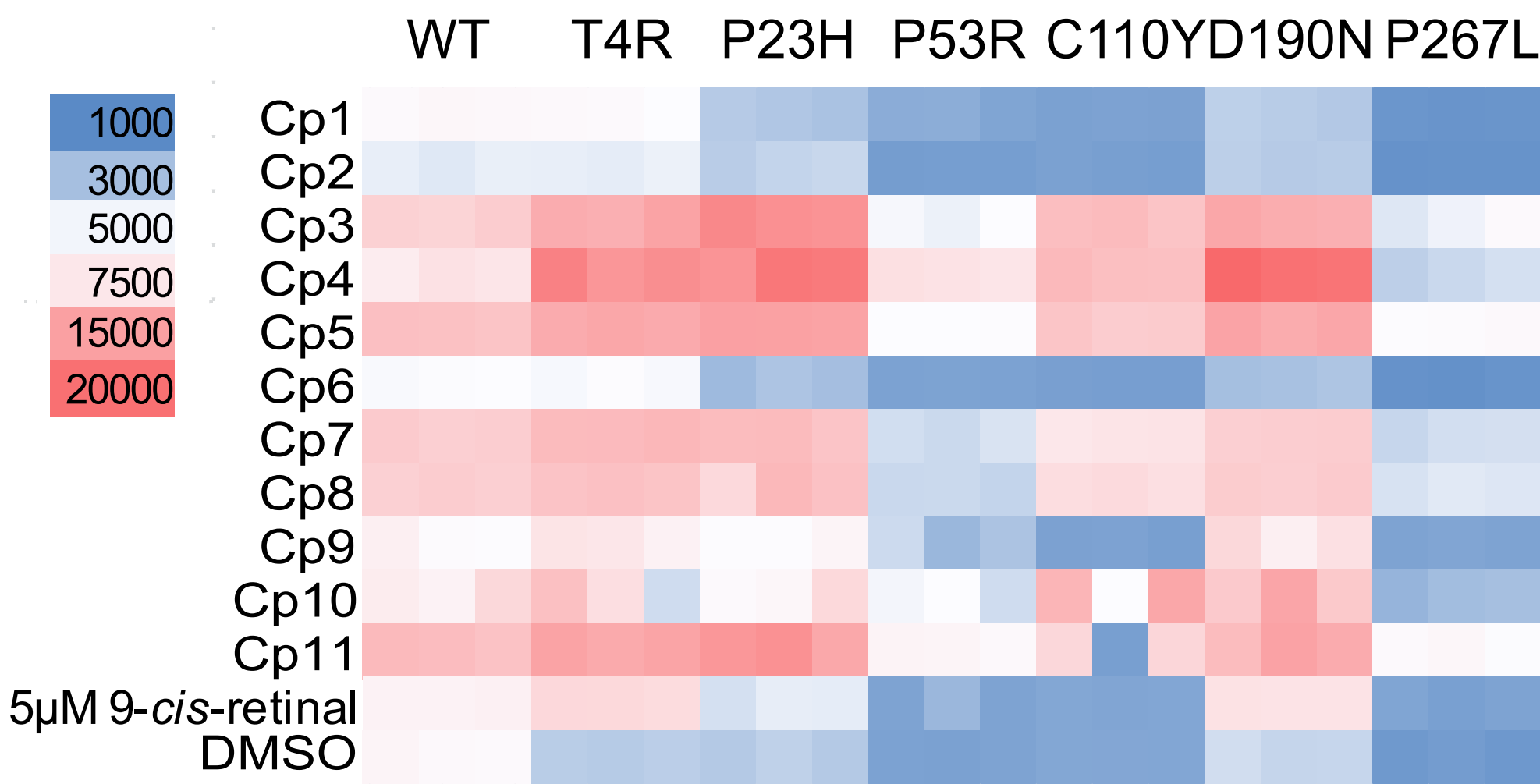


D



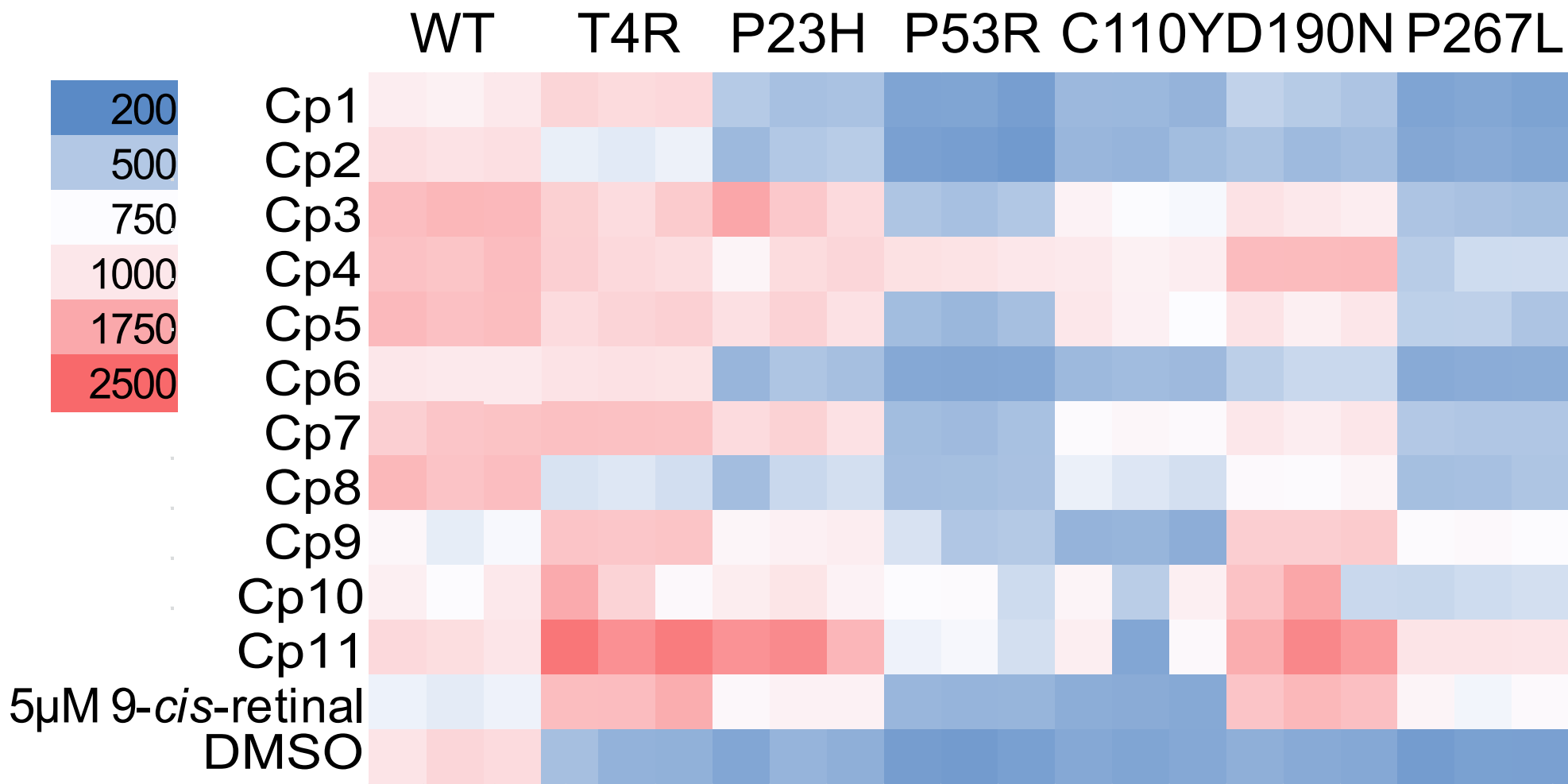
A

Rhodopsin-Venus INT



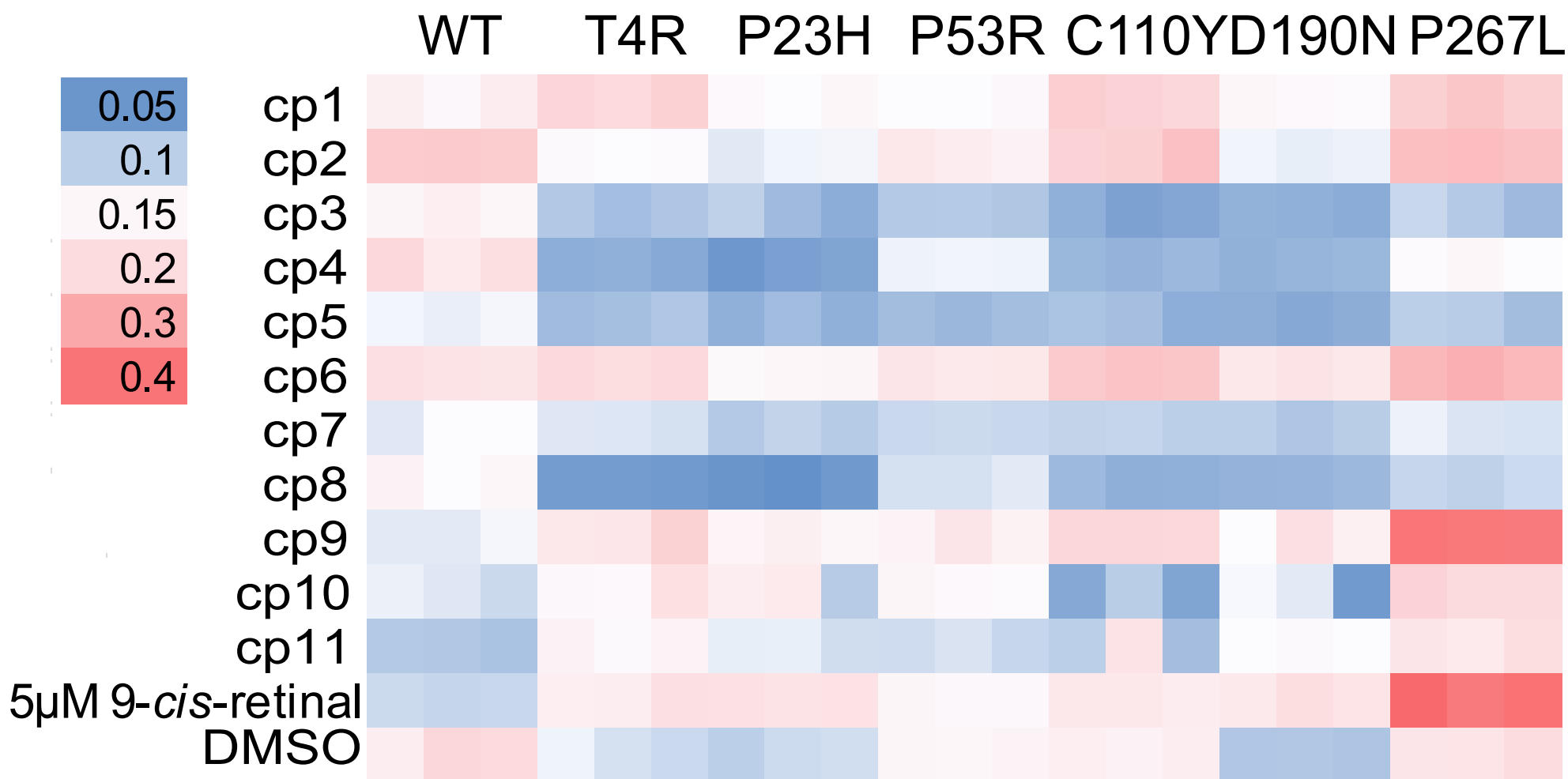
B

Rhodopsin INT on the cell surface



C

MEM-to-Total Ratio



| Name of Material/ Equipment | Company | Catalog Number |
|---|---|----------------|
| U2OS (rhodopsin-Venus) cells | NA | NA |
| U2OS (T4R-rhodopsin-Venus) cells | NA | NA |
| U2OS (P23H-rhodopsin-Venus) cells | NA | NA |
| U2OS (P53R-rhodopsin-Venus) cells | NA | NA |
| U2OS (C110Y-rhodopsin-Venus) cells | NA | NA |
| U2OS (D190N-rhodopsin-Venus) cells | NA | NA |
| U2OS (P267L-rhodopsin-Venus) cells | NA | NA |
| DMEM high glucose | Genesee Scientific | 25-500 |
| Fetal bovine serum (FBS) | Gibco | 16140071 |
| Plasmocin | InvivoGen | ant-mpt |
| Penicillin-Streptomycin (100X) | Gibco | 15140122 |
| Trypsin-EDTA | Genesee Scientific | 25-510 |
| Poly-L-lysine solution | Sigma-Aldrich | P4707-50ML |
| CellCarrier-384 Ultra Microplates | PerkinElmer | 6057300 |
| Sterile 96-well plate | Eppendorf | 30730119 |
| Phosphate Buffered Sialine (PBS) | Invitrogen | AM9625 |
| DMSO | Sigma-Aldrich | D4540 |
| 9- <i>cis</i> -retinal | Sigma-Aldrich | R5754 |
| Compounds tested | Selleckchem/Life Chemicals/Custom synthesized | NA |
| B6-30 anti-rhodopsin antibody | Novus | NBP2-25160 |
| Cy3-conjugated goat anti-mouse secondary antibody | Jackson ImmunoResearch Laboratories, Inc | 115-165-146 |
| 16% paraformaldehyde | Thermo Fisher Scientific | 28908 |
| 10% Normal Goat Serum | Thermo Fisher Scientific | 50062Z |
| Hoechst 33342, Trihydroch | Invitrogen | H3570 |

| | | |
|---|--------------------|--------------|
| High-content imager | Molecular Devices | ImageXpress |
| MetaXpress high-content image acquisition and analysis software | | |
| Multichannel pipette (0.5-10 μ L) | Molecular Devices | MetaXpress |
| Multichannel pipette (0.5-10c | Rainin | 17013802 |
| Electronic multichannel pipette (10-200 μ L) | Rainin | 17013805 |
| 50ml Reagent Reservoir | Thermo Scientific | 14-3879-56BT |
| 8-Channel aspirator | Genesee Scientific | 28-125 |
| Excel spreadsheet software | ABC Scientific | EV503 |
| Origin2018 scientific data analysis and graphing software | Microsoft | Excel2016 |
| | OriginLab | Origin2018 |

Comments/Description

Stable cells generated from U2OS cells

Stable cells generated from U2OS cells

Stable cells generated from U2OS cells

Stable cells generated from U2OS cells

Stable cells generated from U2OS cells

Stable cells generated from U2OS cells

Stable cells generated from U2OS cells

With L-Glutamine, sodium pyruvate

Heat inactivated

Mycoplasma elimination reagent

100X concentrated antibiotic solutions to prevent bacteria contamination of cell cultures

0.25%, 1mM EDTA in HBSS without calcium and magnesium

Mol wt 70,000-150,000, 0.01%, sterile-filtered, BioReagent, suitable for cell culture

384-well tissue culture-treated microplates with black well walls and an optically -clear cyclic olefin bottom for imaging cells in high content analysis

Tissue culture treated with lid flat bottom, sterile, free of detectable pyrogens, RNase, DNase and DNA. Non-cytotoxic

10 x PBS Buffer, pH 7.4

>99.5%, cell culture tested

Compounds were purchased from different vendors or custom synthesized

Gift from Dr. Krzysztof Palczewski

Methanol-free

Blocking buffer

Nuclear staining solution

ImageXpress® Micro Confocal High-Content Imaging System

High-content image acquisition and analysis software

Manual 8-channel pipette, 0.5-10 µL

Manual 8-channel pipette, 20-200 µL

Electronic multichannel pipette for 96- and 384-well microplate pipetting tasks

Reagent reservoir for multichannel pipette dispensing

8-Channel stainless steel adaptor for aspirating liquids from 96- or 384-well plates

The spreadsheet software for data analysis and heatmap generation

The data analysis software for generating the dose response curves



1 Alewife Center #200
Cambridge, MA 02140
tel. 617.945.9051
www.jove.com

ARTICLE AND VIDEO LICENSE AGREEMENT

Title of Article:

The rhodopsin transport and clearance assays by high-content imaging analyses

Author(s):

Bing Feng, Xujie Liu and Yuanyuan Chen

Item 1 (check one box): The Author elects to have the Materials be made available (as described at <http://www.jove.com/author>) via: ☒ Standard Access ☐ Open Access

Item 2 (check one box):

- ☒ The Author is NOT a United States government employee.
- ☐ The Author is a United States government employee and the Materials were prepared in the course of his or her duties as a United States government employee.
- ☐ The Author is a United States government employee but the Materials were NOT prepared in the course of his or her duties as a United States government employee.

ARTICLE AND VIDEO LICENSE AGREEMENT

1. **Defined Terms.** As used in this Article and Video License Agreement, the following terms shall have the following meanings: “**Agreement**” means this Article and Video License Agreement; “**Article**” means the article specified on the last page of this Agreement, including any associated materials such as texts, figures, tables, artwork, abstracts, or summaries contained therein; “**Author**” means the author who is a signatory to this Agreement; “**Collective Work**” means a work, such as a periodical issue, anthology or encyclopedia, in which the Materials in their entirety in unmodified form, along with a number of other contributions, constituting separate and independent works in themselves, are assembled into a collective whole; “**CRC License**” means the Creative Commons Attribution-Non Commercial-No Derivs 3.0 Unported Agreement, the terms and conditions of which can be found at: <http://creativecommons.org/licenses/by-nc-nd/3.0/legalcode>; “**Derivative Work**” means a work based upon the Materials or upon the Materials and other pre-existing works, such as a translation, musical arrangement, dramatization, fictionalization, motion picture version, sound recording, art reproduction, abridgment, condensation, or any other form in which the Materials may be recast, transformed, or adapted; “**Institution**” means the institution, listed on the last page of this Agreement, by which the Author was employed at the time of the creation of the Materials; “**JoVE**” means MyJoVE Corporation, a Massachusetts corporation and the publisher of *The Journal of Visualized Experiments*; “**Materials**” means the Article and / or the Video; “**Parties**” means the Author and JoVE; “**Video**” means any video(s) made by the Author, alone or in conjunction with any other parties, or by JoVE or its affiliates or agents, individually or in collaboration with the Author or any other parties, incorporating all or any portion of the Article, and in which the Author may or may not appear.

2. **Background.** The Author, who is the author of the Article, in order to ensure the dissemination and protection of the Article, desires to have the JoVE publish the Article and create and transmit videos based on the Article. In furtherance of such goals, the Parties desire to memorialize in this Agreement the respective rights of each Party in and to the Article and the Video.

3. **Grant of Rights in Article.** In consideration of JoVE agreeing to publish the Article, the Author hereby grants to JoVE, subject to **Sections 4 and 7** below, the exclusive, royalty-free, perpetual (for the full term of copyright in the Article, including any extensions thereto) license (a) to publish, reproduce, distribute, display and store the Article in all forms, formats and media whether now known or hereafter developed (including without limitation in print, digital and electronic form) throughout the world, (b) to translate the Article into other languages, create adaptations, summaries or extracts of the Article or other Derivative Works (including, without limitation, the Video) or Collective Works based on all or any portion of the Article and exercise all of the rights set forth in (a) above in such translations, adaptations, summaries, extracts, Derivative Works or Collective Works and (c) to license others to do any or all of the above. The foregoing rights may be exercised in all media and formats, whether now known or hereafter devised, and include the right to make such modifications as are technically necessary to exercise the rights in other media and formats. If the “Open Access” box has been checked in **Item 1** above, JoVE and the Author hereby grant to the public all such rights in the Article as provided in, but subject to all limitations and requirements set forth in, the CRC License.

ARTICLE AND VIDEO LICENSE AGREEMENT

4. **Retention of Rights in Article.** Notwithstanding the exclusive license granted to JoVE in **Section 3** above, the Author shall, with respect to the Article, retain the non-exclusive right to use all or part of the Article for the non-commercial purpose of giving lectures, presentations or teaching classes, and to post a copy of the Article on the Institution's website or the Author's personal website, in each case provided that a link to the Article on the JoVE website is provided and notice of JoVE's copyright in the Article is included. All non-copyright intellectual property rights in and to the Article, such as patent rights, shall remain with the Author.

5. **Grant of Rights in Video – Standard Access.** This **Section 5** applies if the "Standard Access" box has been checked in **Item 1** above or if no box has been checked in **Item 1** above. In consideration of JoVE agreeing to produce, display or otherwise assist with the Video, the Author hereby acknowledges and agrees that, Subject to **Section 7** below, JoVE is and shall be the sole and exclusive owner of all rights of any nature, including, without limitation, all copyrights, in and to the Video. To the extent that, by law, the Author is deemed, now or at any time in the future, to have any rights of any nature in or to the Video, the Author hereby disclaims all such rights and transfers all such rights to JoVE.

6. **Grant of Rights in Video – Open Access.** This **Section 6** applies only if the "Open Access" box has been checked in **Item 1** above. In consideration of JoVE agreeing to produce, display or otherwise assist with the Video, the Author hereby grants to JoVE, subject to **Section 7** below, the exclusive, royalty-free, perpetual (for the full term of copyright in the Article, including any extensions thereto) license (a) to publish, reproduce, distribute, display and store the Video in all forms, formats and media whether now known or hereafter developed (including without limitation in print, digital and electronic form) throughout the world, (b) to translate the Video into other languages, create adaptations, summaries or extracts of the Video or other Derivative Works or Collective Works based on all or any portion of the Video and exercise all of the rights set forth in (a) above in such translations, adaptations, summaries, extracts, Derivative Works or Collective Works and (c) to license others to do any or all of the above. The foregoing rights may be exercised in all media and formats, whether now known or hereafter devised, and include the right to make such modifications as are technically necessary to exercise the rights in other media and formats. For any Video to which this Section 6 is applicable, JoVE and the Author hereby grant to the public all such rights in the Video as provided in, but subject to all limitations and requirements set forth in, the CRC License.

7. **Government Employees.** If the Author is a United States government employee and the Article was prepared in the course of his or her duties as a United States government employee, as indicated in **Item 2** above, and any of the licenses or grants granted by the Author hereunder exceed the scope of the 17 U.S.C. 403, then the rights granted hereunder shall be limited to the maximum rights permitted under such

statute. In such case, all provisions contained herein that are not in conflict with such statute shall remain in full force and effect, and all provisions contained herein that do so conflict shall be deemed to be amended so as to provide to JoVE the maximum rights permissible within such statute.

8. **Likeness, Privacy, Personality.** The Author hereby grants JoVE the right to use the Author's name, voice, likeness, picture, photograph, image, biography and performance in any way, commercial or otherwise, in connection with the Materials and the sale, promotion and distribution thereof. The Author hereby waives any and all rights he or she may have, relating to his or her appearance in the Video or otherwise relating to the Materials, under all applicable privacy, likeness, personality or similar laws.

9. **Author Warranties.** The Author represents and warrants that the Article is original, that it has not been published, that the copyright interest is owned by the Author (or, if more than one author is listed at the beginning of this Agreement, by such authors collectively) and has not been assigned, licensed, or otherwise transferred to any other party. The Author represents and warrants that the author(s) listed at the top of this Agreement are the only authors of the Materials. If more than one author is listed at the top of this Agreement and if any such author has not entered into a separate Article and Video License Agreement with JoVE relating to the Materials, the Author represents and warrants that the Author has been authorized by each of the other such authors to execute this Agreement on his or her behalf and to bind him or her with respect to the terms of this Agreement as if each of them had been a party hereto as an Author. The Author warrants that the use, reproduction, distribution, public or private performance or display, and/or modification of all or any portion of the Materials does not and will not violate, infringe and/or misappropriate the patent, trademark, intellectual property or other rights of any third party. The Author represents and warrants that it has and will continue to comply with all government, institutional and other regulations, including, without limitation all institutional, laboratory, hospital, ethical, human and animal treatment, privacy, and all other rules, regulations, laws, procedures or guidelines, applicable to the Materials, and that all research involving human and animal subjects has been approved by the Author's relevant institutional review board.

10. **JoVE Discretion.** If the Author requests the assistance of JoVE in producing the Video in the Author's facility, the Author shall ensure that the presence of JoVE employees, agents or independent contractors is in accordance with the relevant regulations of the Author's institution. If more than one author is listed at the beginning of this Agreement, JoVE may, in its sole discretion, elect not take any action with respect to the Article until such time as it has received complete, executed Article and Video License Agreements from each such author. JoVE reserves the right, in its absolute and sole discretion and without giving any reason therefore, to accept or decline any work submitted to JoVE. JoVE and its employees, agents and independent contractors shall have

ARTICLE AND VIDEO LICENSE AGREEMENT

full, unfettered access to the facilities of the Author or of the Author's institution as necessary to make the Video, whether actually published or not. JoVE has sole discretion as to the method of making and publishing the Materials, including, without limitation, to all decisions regarding editing, lighting, filming, timing of publication, if any, length, quality, content and the like.

11. **Indemnification.** The Author agrees to indemnify JoVE and/or its successors and assigns from and against any and all claims, costs, and expenses, including attorney's fees, arising out of any breach of any warranty or other representations contained herein. The Author further agrees to indemnify and hold harmless JoVE from and against any and all claims, costs, and expenses, including attorney's fees, resulting from the breach by the Author of any representation or warranty contained herein or from allegations or instances of violation of intellectual property rights, damage to the Author's or the Author's institution's facilities, fraud, libel, defamation, research, equipment, experiments, property damage, personal injury, violations of institutional, laboratory, hospital, ethical, human and animal treatment, privacy or other rules, regulations, laws, procedures or guidelines, liabilities and other losses or damages related in any way to the submission of work to JoVE, making of videos by JoVE, or publication in JoVE or elsewhere by JoVE. The Author shall be responsible for, and shall hold JoVE harmless from, damages caused by lack of sterilization, lack of cleanliness or by contamination due to the making of a video by JoVE its employees, agents or independent contractors. All sterilization, cleanliness or decontamination procedures shall be solely the responsibility of the Author and shall be undertaken at the Author's

expense. All indemnifications provided herein shall include JoVE's attorney's fees and costs related to said losses or damages. Such indemnification and holding harmless shall include such losses or damages incurred by, or in connection with, acts or omissions of JoVE, its employees, agents or independent contractors.

12. **Fees.** To cover the cost incurred for publication, JoVE must receive payment before production and publication the Materials. Payment is due in 21 days of invoice. Should the Materials not be published due to an editorial or production decision, these funds will be returned to the Author. Withdrawal by the Author of any submitted Materials after final peer review approval will result in a US\$1,200 fee to cover pre-production expenses incurred by JoVE. If payment is not received by the completion of filming, production and publication of the Materials will be suspended until payment is received.

13. **Transfer, Governing Law.** This Agreement may be assigned by JoVE and shall inure to the benefits of any of JoVE's successors and assignees. This Agreement shall be governed and construed by the internal laws of the Commonwealth of Massachusetts without giving effect to any conflict of law provision thereunder. This Agreement may be executed in counterparts, each of which shall be deemed an original, but all of which together shall be deemed to me one and the same agreement. A signed copy of this Agreement delivered by facsimile, e-mail or other means of electronic transmission shall be deemed to have the same legal effect as delivery of an original signed copy of this Agreement.

A signed copy of this document must be sent with all new submissions. Only one Agreement required per submission.

CORRESPONDING AUTHOR:

Name:

Yuanyuan Chen

Department:

Ophthalmology

Institution:

University of Pittsburgh

Article Title:

The rhodopsin transport and clearance assays by high-content imaging analyses

Signature:

Chen Yuanyuan

Date:

6/29/2018

Please submit a signed and dated copy of this license by one of the following three methods:

- 1) Upload a scanned copy of the document as a pdf on the JoVE submission site;
- 2) Fax the document to +1.866.381.2236;
- 3) Mail the document to JoVE / Attn: JoVE Editorial / 1 Alewife Center #200 / Cambridge, MA 02139

For questions, please email submissions@jove.com or call +1.617.945.9051

Sep 1st, 2018

Dear Dr. Wu,

Thank you for your comments of our manuscript. Here enclosed our revised manuscript. We have addressed all your comments with our responses marked in blue. We look forward to your final decision.

Sincerely,

Yuanyuan Chen, Ph.D.

Editorial comments:

The manuscript has been modified and the updated manuscript, **58703_R1.docx**, is attached and located in your Editorial Manager account. **Please use the updated version to make your revisions.**

1. Please take this opportunity to thoroughly proofread the manuscript to ensure that there are no spelling or grammar issues.

We have proofread the manuscript multiple times to eliminate the spelling and grammar issues.

2. Please do not separate the Protocol section into two parts. Please number the protocol steps continuously.

The protocol now has only one part and is numbers continuously.

3. Please do not number the notes.

Notes are not without numbers.

4. Please reference the notes as superscripts in the manuscript.

Notes are referred as superscripts in the manuscript.

5. Please use h, min, s for time units.

Time units are used as h, min and s.